

Optomechanics with a polarization nondegenerate cavity

F. M. Buters,^{1,*} M. J. Weaver,² H. J. Eerkens,¹ K. Heeck,¹ S. de Man,¹ and D. Bouwmeester^{1,2}

¹*Huygens-Kamerlingh Onnes Laboratorium, Universiteit Leiden, 2333 CA Leiden, The Netherlands*

²*Department of Physics, University of California, Santa Barbara, California 93106, USA*

(Received 23 June 2016; published 5 December 2016)

Experiments in the field of optomechanics do not yet fully exploit the photon polarization degree of freedom. Here experimental results for an optomechanical interaction in a polarization nondegenerate system are presented and schemes are proposed for how to use this interaction to perform accurate side-band thermometry and to create interesting forms of photon-phonon entanglement. The experimental system utilizes the compressive force in the mirror attached to a mechanical resonator to create a micromirror with two radii of curvature which leads, when combined with a second mirror, to a significant polarization splitting of the cavity modes.

DOI: [10.1103/PhysRevA.94.063813](https://doi.org/10.1103/PhysRevA.94.063813)

I. INTRODUCTION

Coupling mechanical motion to electromagnetic radiation lies at the heart of cavity optomechanics. Because the coupling is so general, a wide variety of experiments exist. For example, the scale on which the mechanical motion takes place can range from suspended macroscopic mirrors [1–3] to cold atoms coupled to an optical cavity [4], see Ref. [5] for a review. Also, the source of electromagnetic radiation varies greatly, ranging from the microwave [6,7] to the optical domain [8–11]. Each device and setup has its own advantages. In the optical domain, the availability of the polarization degree of freedom adds an additional knob for controlling and tuning the optomechanical devices. This means that techniques and methods from several landmark experiments demonstrating photon-photon [12,13] or photon-matter [14,15] entanglement can be implemented in existing optomechanical setups. However, so far, polarization has mostly been used to experimentally separate different optical signals and is not yet considered as a degree of freedom in, e.g., proposals [16–20] and experiments [21,22] on photon-phonon entanglement.

This is understandable since the mechanical mode in an optomechanical system is not sensitive to the polarization of the incoming photon. However, the optical mode can be engineered to be polarization sensitive. Birefringence or astigmatism can cause a polarization splitting of the (fundamental) mode of an optical cavity. Although such birefringence has been observed before in optomechanical setups, it has been regarded as a parasitic effect [23,24]. In this article we show an optomechanical system in which a significant polarization splitting of the fundamental mode is present. After a brief characterization of the setup we show how, for a single laser frequency, the interaction can be changed from cooling to driving simply by varying the polarization. Finally, some advantages of a polarization nondegenerate optomechanical system are discussed.

II. EXPERIMENTAL DETAILS

In a Fabry–Perot-based system, birefringence occurs when one cavity mirror, either the stationary or the movable mirror,

has two radii of curvature. We chose to use the curvature already present in the mirror attached to a trampoline resonator. The trampoline resonator consists of multiple distributed Bragg reflector (DBR) layers on top of a patterned silicon nitride membrane [see inset of Fig. 1(a)]. Finite element analysis using COMSOL shows that the compressive force in the DBR mirror is much larger than the tensile force in the silicon nitride, causing the mirror to buckle slightly. This is schematically depicted in Fig. 1(a). We have confirmed the mirror curvature with an optical profiler. Figure 1(b) shows a concave mirror surface. Such small high-quality curved mirrors are already interesting on their own to make small microcavities for cavity QED experiments. For a polarization nondegenerate cavity, however, an astigmatic mirror is needed.

Closer inspection of the mirror surface reveals a four-fold symmetry for the curvature in the center of the mirror, as expected from the geometry of the trampoline resonator. Because the DBR mirror is oversized, 110 μm diameter, compared with the beam size, typically 12 μm diameter, a high-quality cavity can still be constructed by placing the beam off axis. It is therefore interesting to look at the local curvature away from the middle. For the white dot in Fig. 1(b), we determine the local radius of curvature (ROC) by fitting a parabola to a line cut straight through the center of the white dot [see dashed line Fig. 1(b)]. From the derivative of the parabola the ROC is obtained [25]. If we repeat this procedure for line cuts at different angles we obtain Fig. 1(c). A clear twofold symmetry is present, with a minimum ROC of about 1 mm and a maximum ROC of about 4 mm. Using these numbers together with the recently published work by Uphoff *et al.* [26], a polarization splitting of about 60 kHz for the fundamental mode is expected based on the parameters of the setup.

To demonstrate such a splitting, a 5-cm-long Fabry–Perot cavity operating around 1064 nm is placed in a vibration-isolated vacuum chamber. In this configuration the convex side of the trampoline resonator faces the stationary mirror. The fundamental mode of the cavity is aligned such that the cavity mode is located on the side of the small curved mirror. The optical quality factor is constant with respect to beam placement; only near the very edge of the mirror does the optical quality degrade due to clipping of the beam. Both beam placement and optical quality factor are actively monitored during alignment to prevent this clipping of the beam. Via a

*buters@physics.leidenuniv.nl

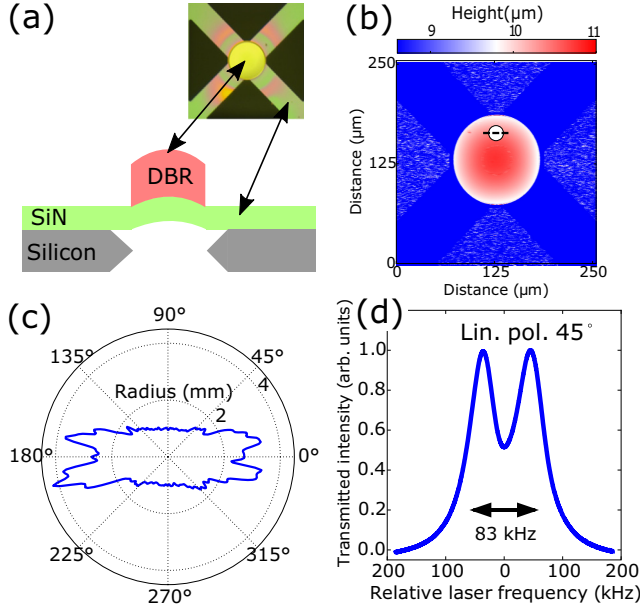


FIG. 1. (a) Compressive stress in the DBR layers causes the mirror to buckle. Inset shows optical image of the trampoline resonator. (b) Optical profiling with a confocal microscope reveals a concave mirror surface. (c) Local radius of curvature as function of angle obtained for the off-center location indicated with the white dot in panel (b). (d) Demonstration of mode splitting for an off-axis-aligned cavity by monitoring the transmitted intensity when the laser frequency is varied.

cavity ringdown [27] the optical linewidth is determined to be 51 ± 1 kHz and the mechanical resonator is characterized by measuring its mechanical thermal noise spectrum with a laser locked to a cavity resonance by using the Pound–Drever–Hall (PDH) technique [28]. With this technique an intrinsic mechanical linewidth Γ_m of 19 Hz and a mechanical frequency Ω_m of 222 kHz is measured.

III. RESULTS

To see if any polarization splitting is present, a laser is scanned across the cavity resonance and the input polarization is adjusted to address both polarization modes equally. A polarization splitting of 83 ± 1.0 kHz is observed, as shown in Fig. 1(d). This is of the same order as the expected polarization splitting of 60 kHz. Furthermore, the splitting is large enough to already show some interesting optomechanical effects. For this, the measurement scheme outlined in Ref. [27] is used. A probe laser at the cavity resonance is used to monitor the mechanical motion while the detuning of a second pump laser is varied.

For each specific laser detuning we measure the mechanical noise spectrum, fit a Lorentzian, and extract the mechanical linewidth and frequency. The results are shown in Fig. 2. Note that the laser detuning is indicated for one of the two optical modes. The detuning for the other mode is shifted by 83 kHz, the polarization splitting. Since our optomechanical system operates in the linearized regime, the frequency shift and effective damping can be understood by adding the

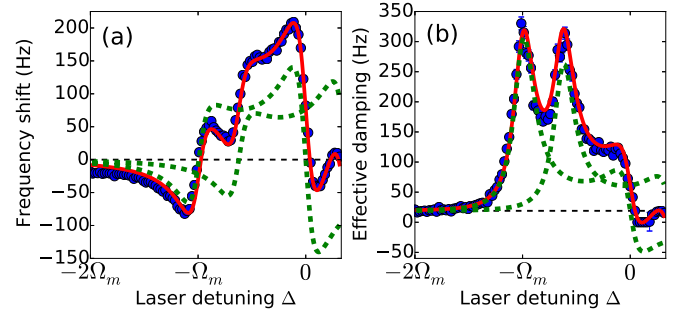


FIG. 2. Optomechanical interaction for a polarization nondegenerate cavity. Blue points are extracted from the Lorentzian fit to the mechanical resonance. Red is a simultaneous fit of the data with four free parameters: optical linewidth, optical splitting, and input laser power for both modes. Green shows the contribution of the individual modes. Panel (a) shows the mechanical frequency shift and panel (b) shows the effective mechanical damping.

contributions of both modes:

$$\delta\Omega_{m,\text{total}} = \delta\Omega_{m,1} + \delta\Omega_{m,2}, \quad (1)$$

$$\Gamma_{\text{eff},\text{total}} = \Gamma_{\text{opt},1} + \Gamma_{\text{opt},2} + \Gamma_m, \quad (2)$$

where $\delta\Omega_{m,i}$ and $\Gamma_{\text{opt},i}$ are the optically induced frequency shift and damping (see, for example, Ref. [5] for detailed expressions). In green is shown the individual contribution from each mode and in red is shown the result of a fit for the combined effect of both modes. Note that the red curve in Figs. 2 and 3 is obtained from a single simultaneous fit to all data with only four free parameters: the optical linewidth, the mode splitting, and the input power of both the horizontal and vertical polarization modes. From Fig. 2 we see that the experimental results are nicely described by the addition of the two separate contributions. Furthermore, we obtain an optical linewidth κ of 52 ± 0.9 kHz, a mode splitting of 82.4 ± 1.2 kHz, and an input laser power of $2.19 \pm 0.04 \mu\text{W}$ and $1.85 \pm 0.04 \mu\text{W}$ for both optical modes. These results are in good agreement with the optical characterization. It is also clear that, at $\Delta = 41.5$ kHz, precisely between both optical modes, their contributions cancel.

This is even more clear when looking at the effective temperature of the mechanical mode, which is obtained from

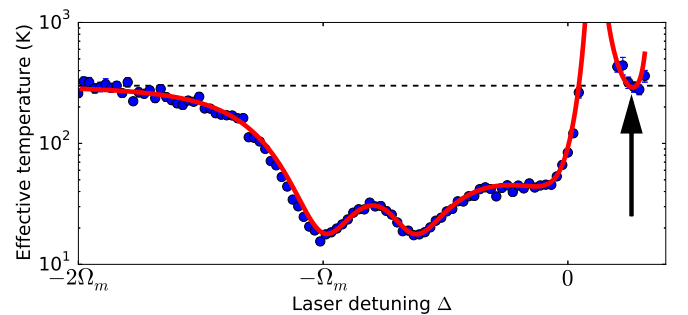


FIG. 3. Effective temperature as a function of laser detuning. The arrow indicates the point where the contribution from both modes precisely cancel each other, leading to an effective temperature equal to the bath temperature.

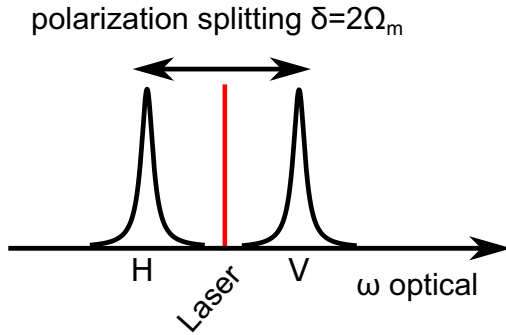


FIG. 4. A polarization nondegenerate cavity with a splitting $\delta = 2\Omega_m$. H and V denote the different polarization and corresponding cavity mode.

the area of the Lorentzian fit to the mechanical resonance. The theory curve for Fig. 3 is given by

$$T_{\text{eff}} = \frac{\hbar\Omega_m \bar{n}_{\text{th}}\Gamma_m + \bar{n}_{\text{min}}\Gamma_{\text{opt}}}{k_B (\Gamma_m + \Gamma_{\text{opt}})}, \quad (3)$$

with $\bar{n}_{\text{min}} = (\kappa/4\Omega_m)^2$ being the theoretical minimum phonon number in the side-band resolved regime and \bar{n}_{th} being the thermal phonon occupation number. For the optical damping Γ_{opt} we use the sum of the contributions from both modes [see Eq. (2)]. From the resulting graph of Fig. 3 we see again that the experimental results follow the theory nicely. Furthermore, at laser detuning $\Delta = 41.5$ kHz indicated by the arrow, the effective mode temperature is just the environmental temperature, showing once more that the contribution from both polarization modes cancel out. However, if the laser is kept at $\Delta = 41.5$ kHz and the input polarization is changed, one mode will dominate, leading to either heating or cooling.

Of course the same effect can be obtained by using two lasers placed at either side of the cavity resonance, or perhaps even by using higher-order optical modes, but using the polarization degree of freedom as described above has several advantages. Because only a single frequency is used, the whole setup has one common path, which improves the stability of the experiment. Second, one single narrow-linewidth laser frequency is needed. Furthermore, only the fundamental Gaussian transverse mode is required, which has the same optical quality for both polarization modes. Finally, the power ratio between the two modes is easily adjusted simply by rotating the incident polarization.

In principle these advantages are only technical. There are however interesting opportunities when the polarization splitting is precisely two times the mechanical frequency. For example, an alternative method for side-band thermometry [29–33], which is the optomechanical equivalent to Raman-ratio thermometry in cold atoms [34] and solids [35], is possible. In Fig. 4, a laser, 45° linearly polarized, is placed precisely in the middle of the two polarization modes. Interaction with the horizontal mode leads to Stokes scattering, while interaction with the vertical mode leads to anti-Stokes scattering. For a large average phonon number $\langle n \rangle$ both the horizontal mode (Stokes sideband) and vertical mode (anti-Stokes sideband) will exit the cavity with equal intensity.

However, when the phonon occupation number is lowered, Stokes scattering becomes dominant and the light exiting the cavity will be mainly in the horizontal mode. Therefore, the phonon number can be accurately obtained by measuring the ratio of transmitted light in the horizontal and vertical mode, since this will scale as $1 + 1/\langle n \rangle$.

Another interesting opportunity arises when a polarization nondegenerate system is prepared in the quantum-mechanical ground state, a prerequisite for photon-phonon entanglement. Often a beam splitter is used to create photon-photon entanglement [16–20]. For a polarization-sensitive cavity this is no longer needed. If we again consider the situation of Fig. 4 but replace the laser with a single-photon source, we see that entanglement arises when the incoming photon, 45° linearly polarized, is projected onto either basis state. By projecting onto the horizontal basis state, a phonon will be added to the mechanical resonator, while projecting onto the vertical basis state will extract a phonon. When, for example, starting from the $\langle n \rangle = 1$ state, the mechanical resonator is put into a superposition between the ground state and the second-excited state. This is not possible when a beam splitter is used together with multiple laser frequencies. The addition of the polarization degree of freedom has created a non-trivial method to manipulate the state of the mechanical resonator. Furthermore, additional tools from the polarization-quantum optics toolbox can now be used. The input photon can be replaced with polarization-entangled photon pairs, where one photon interacts with the resonator while the state of the other photon is monitored. We must, however, remark that, for such single-photon experiments, either single-photon strong coupling is required or a postselection method has to be implemented [36].

To access this interesting regime, a system with a polarization splitting of two times the mechanical frequency is needed. This requires only a small modification to the system presented here. Fabry–Perot-based optomechanical systems are available with an optical linewidth smaller than 17 kHz, a mechanical frequency of 250 kHz, and a mechanical quality factor approaching 5×10^5 [37]. Taking this as a starting point, a cavity with a mode splitting of 500 kHz is needed. With some small modifications to the trampoline resonator design, the mode splitting can be pushed from 83 to about 100 kHz. Since the mode splitting scales inversely with cavity length [26], reducing the cavity length by a factor of five results in the desired mode splitting. This will also increase the optomechanical coupling strength g_0 to about $2\pi \times 8$ rad/s. A downside to this method is that the cavity linewidth increases by a factor of five, but an optical linewidth of 85 kHz is still sufficient to be side-band resolved. More importantly, to achieve ground-state cooling, the multiphoton cooperativity should be much larger than the thermal occupation number. In this case a base temperature of 1 K together with a laser power of $50 \mu\text{W}$ is needed, which is experimentally feasible.

IV. CONCLUSION

In conclusion, we have shown how a polarization nondegenerate optomechanical system can be a valuable addition to the existing optomechanical toolbox. We have created

a system where optomechanical interaction with a single-frequency laser can be tuned from cooling to heating simply by varying the incident polarization. On its own this offers some technical advantages but, combined with an optomechanical system close to the quantum ground state, this leads to interesting possibilities for photon-phonon entanglement. We have demonstrated how such a system can be fabricated and showed that the last remaining step is to decrease the length to bring the presented system into the target regime.

ACKNOWLEDGMENTS

The authors acknowledge useful discussions with W. Loeffler. The authors would also like to thank H. van der Meer for technical assistance and support. This work is part of the research program of the Foundation for Fundamental Research (FOM) and of the NWO VICI research program, which are both part of the Netherlands Organization for Scientific Research (NWO). This work is also supported by the National Science Foundation Grant No. PHY-1212483.

-
- [1] T. Corbitt, Y. Chen, E. Innerhofer, H. Müller-Ebhardt, D. Ottaway, H. Rehbein, D. Sigg, S. Whitcomb, C. Wipf, and N. Mavalvala, *Phys. Rev. Lett.* **98**, 150802 (2007).
- [2] A. Borrielli, A. Pontin, F. S. Cataliotti, L. Marconi, F. Marin, F. Marino, G. Pandraud, G. A. Prodi, E. Serra, and M. Bonaldi, *Phys. Rev. Appl.* **3**, 054009 (2015).
- [3] J. C. Sankey, C. Yang, B. M. Zwickl, A. M. Jayich, and J. G. Harris, *Nat. Phys.* **6**, 707 (2010).
- [4] D. W. Brooks, T. Botter, S. Schreppler, T. P. Purdy, N. Brahms, and D. M. Stamper-Kurn, *Nature (London)* **488**, 476 (2012).
- [5] M. Aspelmeyer, T. J. Kippenberg, and F. Marquardt, *Rev. Mod. Phys.* **86**, 1391 (2014).
- [6] J. Teufel, T. Donner, D. Li, J. Harlow, M. Allman, K. Cicak, A. Sirois, J. Whittaker, K. Lehnert, and R. Simmonds, *Nature (London)* **475**, 359 (2011).
- [7] V. Singh, S. J. Bosman, B. H. Schneider, Y. M. Blanter, A. Castellanos-Gomez, and G. A. Steele, *Nat. Nanotechnol.* **9**, 820 (2014).
- [8] J. Chan, T. M. Alegre, A. H. Safavi-Naeini, J. T. Hill, A. Krause, S. Gröblacher, M. Aspelmeyer, and O. Painter, *Nature (London)* **478**, 89 (2011).
- [9] S. Weis, R. Rivière, S. Deléglise, E. Gavartin, O. Arcizet, A. Schliesser, and T. J. Kippenberg, *Science* **330**, 1520 (2010).
- [10] S. Gröblacher, K. Hammerer, M. R. Vanner, and M. Aspelmeyer, *Nature (London)* **460**, 724 (2009).
- [11] X.-Y. Lü, Y. Wu, J. R. Johansson, H. Jing, J. Zhang, and F. Nori, *Phys. Rev. Lett.* **114**, 093602 (2015).
- [12] A. Aspect, J. Dalibard, and G. Roger, *Phys. Rev. Lett.* **49**, 1804 (1982).
- [13] J.-W. Pan, M. Daniell, S. Gasparoni, G. Weihs, and A. Zeilinger, *Phys. Rev. Lett.* **86**, 4435 (2001).
- [14] E. Togan, Y. Chu, A. Trifonov, L. Jiang, J. Maze, L. Childress, M. G. Dutt, A. S. Sørensen, P. Hemmer, A. Zibrov *et al.*, *Nature (London)* **466**, 730 (2010).
- [15] W. Gao, P. Fallahi, E. Togan, J. Miguel-Sánchez, and A. Imamoglu, *Nature (London)* **491**, 426 (2012).
- [16] W. Marshall, C. Simon, R. Penrose, and D. Bouwmeester, *Phys. Rev. Lett.* **91**, 130401 (2003).
- [17] M. Paternostro, D. Vitali, S. Gigan, M. S. Kim, C. Brukner, J. Eisert, and M. Aspelmeyer, *Phys. Rev. Lett.* **99**, 250401 (2007).
- [18] D. Vitali, S. Gigan, A. Ferreira, H. R. Böhm, P. Tombesi, A. Guerreiro, V. Vedral, A. Zeilinger, and M. Aspelmeyer, *Phys. Rev. Lett.* **98**, 030405 (2007).
- [19] S. G. Hofer, W. Wieczorek, M. Aspelmeyer, and K. Hammerer, *Phys. Rev. A* **84**, 052327 (2011).
- [20] P. Sekatski, M. Aspelmeyer, and N. Sangouard, *Phys. Rev. Lett.* **112**, 080502 (2014).
- [21] T. Palomaki, J. Teufel, R. Simmonds, and K. Lehnert, *Science* **342**, 710 (2013).
- [22] R. Riedinger, S. Hong, R. A. Norte, J. A. Slater, J. Shang, A. G. Krause, V. Anant, M. Aspelmeyer, and S. Gröblacher, *Nature (London)* **530**, 313 (2016).
- [23] S. Gröblacher, J. B. Hertzberg, M. R. Vanner, G. D. Cole, S. Gigan, K. Schwab, and M. Aspelmeyer, *Nat. Phys.* **5**, 485 (2009).
- [24] A. Jayich, J. Sankey, A. Petrenko, and J. Harris, in *Quantum Electronics and Laser Science Conference* (Optical Society of America, Rochester, 2011), p. QThM3.
- [25] E. Kreyszig, *Differential Geometry* (Dover Publications, Mineola, New York, 1991).
- [26] M. Uphoff, M. Brekenfeld, G. Rempe, and S. Ritter, *New J. Phys.* **17**, 013053 (2015).
- [27] H. Eerkens, F. Buters, M. Weaver, B. Pepper, G. Welker, K. Heeck, P. Sonin, S. de Man, and D. Bouwmeester, *Opt. Express* **23**, 8014 (2015).
- [28] E. D. Black, *Am. J. Phys.* **69**, 79 (2001).
- [29] A. Schliesser, O. Arcizet, R. Riviere, G. Anetsberger, and T. Kippenberg, *Nat. Phys.* **5**, 509 (2009).
- [30] A. H. Safavi-Naeini, J. Chan, J. T. Hill, T. P. M. Alegre, A. Krause, and O. Painter, *Phys. Rev. Lett.* **108**, 033602 (2012).
- [31] A. J. Weinstein, C. U. Lei, E. E. Wollman, J. Suh, A. Metelmann, A. A. Clerk, and K. C. Schwab, *Phys. Rev. X* **4**, 041003 (2014).
- [32] T. P. Purdy, P.-L. Yu, N. S. Kampel, R. W. Peterson, K. Cicak, R. W. Simmonds, and C. A. Regal, *Phys. Rev. A* **92**, 031802 (2015).
- [33] M. Underwood, D. Mason, D. Lee, H. Xu, L. Jiang, A. B. Shkarin, K. Børkje, S. M. Girvin, and J. G. E. Harris, *Phys. Rev. A* **92**, 061801 (2015).
- [34] F. Diedrich, J. C. Bergquist, W. M. Itano, and D. J. Wineland, *Phys. Rev. Lett.* **62**, 403 (1989).
- [35] T. Hart, R. Aggarwal, and B. Lax, *Phys. Rev. B* **1**, 638 (1970).
- [36] B. Pepper, R. Ghobadi, E. Jeffrey, C. Simon, and D. Bouwmeester, *Phys. Rev. Lett.* **109**, 023601 (2012).
- [37] M. J. Weaver, B. Pepper, F. Luna, F. M. Buters, H. J. Eerkens, G. Welker, B. Perock, K. Heeck, S. de Man, and D. Bouwmeester, *Appl. Phys. Lett.* **108**, 033501 (2016).